Selected for a Viewpoint in *Physics*

RAPID COMMUNICATIONS

PHYSICAL REVIEW B **80**, 180510(R) (2009)

Band- and momentum-dependent electron dynamics in superconducting $Ba(Fe_{1-x}Co_x)_2As_2$ as seen via electronic Raman scattering

B. Muschler,[1] W. Prestel,[1] R. Hackl,[1] T. P. Devereaux,[2] J. G. Analytis,[2,3] Jiun-Haw Chu,[2,3] and I. R. Fisher[2,3]

[1]*Walther Meissner Institut, Bayerische Akademie der Wissenschaften, 85748 Garching, Germany*

[2]*Stanford Institute for Materials and Energy Sciences, SLAC National Accelerator Laboratory, 2575 Sand Hill Road, Menlo Park, Standford, California 94025, USA*

[3]*Geballe Laboratory for Advanced Materials and Department of Applied Physics, Stanford University, California 94305, USA*

(Received 26 October 2009; published 30 November 2009)

We present details of carrier properties in high quality $Ba(Fe_{1-x}Co_x)_2As_2$ single crystals obtained from electronic Raman scattering. The experiments indicate a strong band and momentum anisotropy of the electron dynamics above and below the superconducting transition, highlighting the importance of complex band-dependent interactions. The presence of low-energy spectral weight deep in the superconducting state suggests a gap with accidental nodes, which may be lifted by doping and/or impurity scattering. When combined with other measurements, our observation of band- and momentum-dependent carrier dynamics indicate that the iron arsenides may have several competing superconducting ground states.

DOI: 10.1103/PhysRevB.80.180510 PACS number(s): 74.25.Gz, 74.20.Mn, 78.30.−j

The high-temperature iron-arsenide (FeAs) superconductors [Fig. 1(a)] (Refs. 1 and 2) exhibit a similar proximity of ground states[2–5] as some heavy-fermion systems and the copper-oxygen compounds. In particular, the proximity of the parent antiferromagnetic to the optimal superconducting phase suggests that the copper-oxygen compounds and the iron arsenides may be cousins in the same family. However, the strong metallicity of the parent phase and the lack of spectral redistribution upon doping observed by angle-resolved photoemission (ARPES) and x-ray absorption in FeAs argue otherwise.[6,7] But perhaps one of the most telling similarities would be if the iron arsenides had the signature property of all cuprates: an energy gap $\Delta_{\mathbf{k}}$ having nodes and a sign change along the Fermi surface.[8]

In the iron arsenides, T_c and the superconducting gap structure have shown a remarkable dependence on the material class and on doping. The magnetic penetration depth $\lambda(T)$ clearly indicates nodes in LaFePO (Refs. 9 and 10) and in the $BaFe_2As_2$ family.[11,12] In $SmFeAsO_{1-x}F_y$, the small finite gaps derived from $\lambda(T)$ (Ref. 13) indicate either strongly anisotropic gaps or gaps that vary significantly between the different Fermi-surface sheets as seen in ARPES in $Ba_{1-x}K_xFe_2As_2$ (Ref. 14) and $Ba(Fe_{1-x}Co_x)_2As_2$.[15] Small but finite gaps are also derived from recent measurements of the thermal conductivity in $Ba(Fe_{1-x}Co_x)_2As_2$ at very low temperatures.[16] As an open experimental issue, surface sensitive point-contact spectroscopy and ARPES experiments generally observe full gaps,[14,15,17–19] whereas bulk sensitive nuclear-magnetic-resonance experiments so far found only indications of gaps with nodes.[20,21] While on one hand, polar surfaces (which may distort the nature of the pair state close to the surface from that of the bulk) may account for the differences between bulk and surface methods, it is also an intriguing possibility that different FeAs superconductors may have different superconducting ground states, such as $s_{\pm}$ or d-wave, which may be selected by small changes in materials chemistry.

In this study, we use bulk and band sensitive inelastic (Raman) light scattering to gain insight into electron dynamics and structures of the gaps. Photons are scattered off of electrons by creating particle-hole pairs across the Fermi level in the normal state or by breaking Cooper pairs in the superconducting state.[22] By changing incident and scattered light polarizations, electron dynamics and the superconducting energy gap can be highlighted in different momentum regions in the BZ [see Fig. 1(b)]. Since the bands lie at high-symmetry points in the BZ B_{2g}, (xy) predominantly probes the β bands, and B_{1g} (x^2-y^2) does not couple strongly to any band. While the A_{1g} (x^2+y^2) vertex in principle probes both bands the largest contribution represents interband scattering involving the α bands, modified by charge backflow effects.

The single crystals of electron-doped $Ba(Fe_{1-x}Co_x)_2As_2$ with $x=0.061(2)$ and $x=0.085(2)$ were synthesized using a self-flux technique and have been characterized elsewhere.[23]

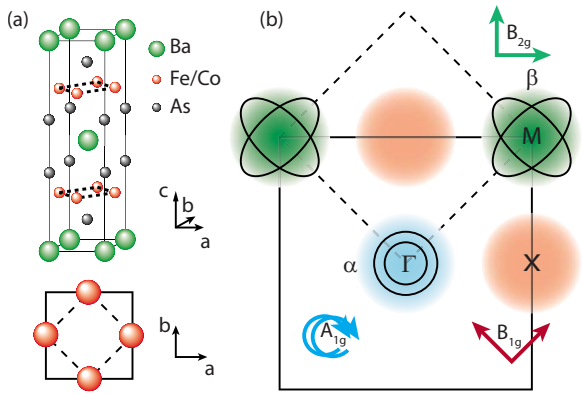

FIG. 1. (Color online) Crystal structure and Raman selection rules for $BaFe_2As_2$. (a) The relevant cell of the Fe plane is smaller by a factor of 2 and is rotated by 45° (dashes) with respect to the crystal cell (full line). (b) Brillouin zone (BZ) of the unit cell (full line) and first quadrant of the Fe plane (dashed line). The light polarizations are indicated symbolically with respect to the basal plane shown in panel (a). The electronic A_{1g} and B_{2g} spectra project the α and β bands, respectively.

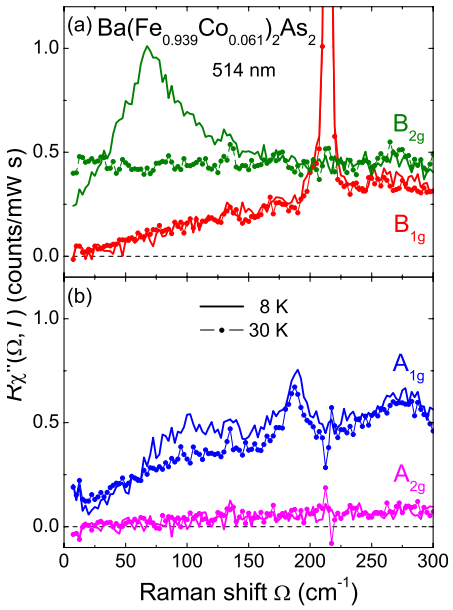

FIG. 2. (Color online) Symmetry-dependent Raman response $R\chi''(\Omega,T)$ of $Ba(Fe_{0.939}Co_{0.061})_2As_2$. (a) In B_{1g} symmetry, there is a phonon at 214 cm^{-1} from Fe vibrations. (b) In A_{1g}, there is a small increase toward $\Omega \to 0$ since it is always measured with parallel polarizations, where the laser is less efficiently suppressed. The analysis demonstrates that the A_{2g} signal can safely be neglected (Ref. 25).

The cobalt concentration was determined by microprobe analysis. At 6.1% and 8.5% dopings, the structural and magnetic transitions have been suppressed below the superconducting transition at T_c=24 K and 22 K, respectively, with $\Delta T_c < 1$ K. The resistivity varies essentially linearly between T_c and 300 K.

In Fig. 2, we plot the spectra $R\chi''$ measured on $Ba(Fe_{0.939}Co_{0.061})_2As_2$ for the four distinct in-plane symmetries, which are linear combinations of the spectra measured at the principal polarizations. We show spectra at 8 K for the superconducting state and at 30 K for the normal state. There is a strong dependence on symmetry in either state, indicated by the differences in the overall spectral line shape and intensity, but also by the different temperature dependences.[24]

The B_{2g} spectra [Fig. 2(a)] are strikingly different from those in the A_{1g} and B_{1g} symmetries. In the normal state, the flat electronic continuum is similar to that in the cuprates[22] and changes strongly with temperature.[24] This indicates that the electrons in the β bands scatter dynamically from excitations. In contrast, the A_{1g}, B_{1g}, and A_{2g} symmetries (Fig. 2) yield suppressed practically temperature-independent spectra.[24] This strong polarization dependence implies that the charge-carrier relaxation on the α bands (A_{1g}) is fundamentally different from that on the β bands (B_{2g}) and indicates strongly anisotropic- and band-dependent electron interactions.

These polarization dependences carry through into the superconducting state, indicating a marked difference of light scattering from Cooper pairs on the α and β bands (Fig. 2). While for B_{1g} symmetry there is no difference between the normal and superconducting states, for B_{2g} a strong peak at around 70 cm^{-1} and a suppression of spectral weight below 30 cm^{-1} develop below T_c. Here, the peak intensity and its resolution-limited sharpness [see Figs. 3(e) and 3(f)] emphasize the high purity and order of the sample used. The A_{1g} spectra below T_c [Fig. 2(b)] reach a broad maximum close to 100 cm^{-1}. This higher-energy scale indicates a larger gap amplitude on the α bands than on the β bands. The maximum at 100 cm^{-1} or $6k_BT_c$ is consistent with the photoemission results.[14,15]

The redistribution of spectral weight and the peak structures are reminiscent of the superconductivity-induced features in the A15 compounds and in overdoped cuprates.[22] However, unlike the A15's, and more like the cuprates, the finite intensity observed down to very small Raman shifts is

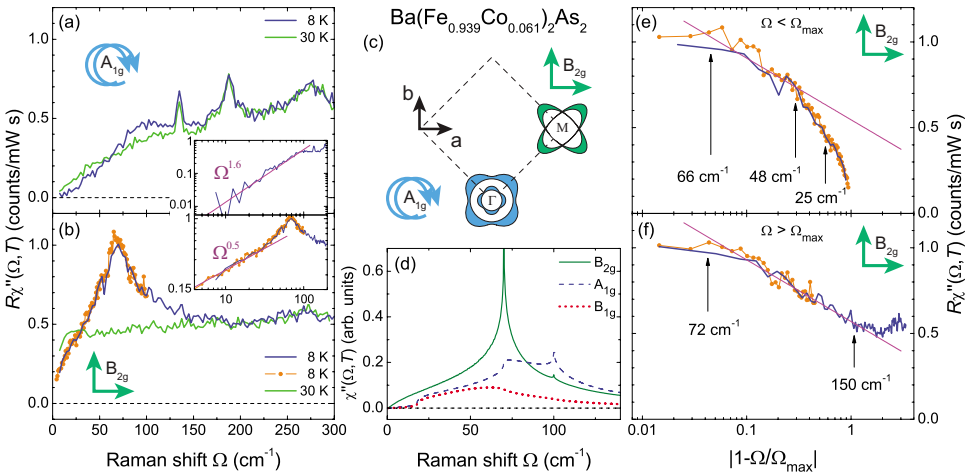

FIG. 3. (Color online) Raman response $R\chi''(\Omega,T)$ of $Ba(Fe_{0.939}Co_{0.061})_2As_2$ in (a) A_{1g} and (b) B_{2g} polarizations. Spectra plotted with full lines are measured with a resolution of 5.0 cm^{-1}. For further clarifying the spectral shape at low energy and around the maximum, the superconducting B_{2g} spectra were also measured with a resolution of 3.6 cm^{-1} [(orange) points in (b), (e), and (f)]. The insets indicate power-law behavior for both symmetries. The finite spectral intensity at low energies supports gap nodes. (c) shows the gap forms used for the Raman spectra calculated in (d). The A_{1g} and B_{1g} spectra are multiplied by 0.5 and 10, respectively. (e) and (f) show the B_{2g} spectra above and below the peak maximum on a logarithmic scale to highlight the divergence around Ω_{max}=69 cm^{-1}.

a clear indication of vanishingly small gaps, where Cooper pairs can be broken with arbitrarily low energies.

In Figs. 3(a) and 3(b), we show the A_{1g} and B_{2g} spectra in greater detail. Both do not show a clear activation threshold but finite intensity down to arbitrarily small Raman shifts, favoring the presence of nodes rather than full gaps on at least some of the bands. Below 80 cm^{-1}, the A_{1g} intensity varies faster than linear following $\Omega^{1.6}$ [inset of Fig. 3(a)]. If there is a threshold, it must be smaller than 30 cm^{-1}. This would translate into a minimal gap $\Delta_{min} \leq 2$ meV or $0.9k_BT_c$ much smaller than that observed by ARPES.[14] Importantly, the B_{2g} spectrum [Fig. 3(b)] varies approximately as $\sqrt{\Omega}$ with a potential threshold below 5 cm^{-1}, suggesting the presence of accidental gap nodes.

The different power laws for A_{1g} and B_{2g} indicate a sensitivity of the pairing gap to the Fermi-surface location, area, and, perhaps, geometry. The low-frequency power laws of the Raman response follow from the density of states (DOS) unless the nodes of the Raman vertices happen to be aligned with the nodes of the gap, as in the case of the B_{1g} channel in the cuprates,[22] imparting a higher power law than that expected from the DOS alone. Since no nodes of the vertex are required by symmetry on the β bands, the $\sqrt{\Omega}$ behavior in the B_{2g} channel argues strongly for a superconducting gap vanishing quadratically with momentum near the nodes. This is the case for an s-wave pair state having accidental nodes [see Fig. 3(c) and Ref. 24].

On the α bands, there are no nodes of the Raman vertices either. Therefore, the observed $\Omega^{1.6}$ dependence of the intensity for the A_{1g} response cannot originate from an interplay between the nodal structure of the gap and the vertices; rather it most likely reflects a threshold broadened by incoherent scattering. These considerations show that there is no universal superconducting energy gap. Rather, there is a substantial variation for the different sheets of the Fermi surface as well as a strong momentum dependence on the individual sheets. Hence, bulk spectroscopic methods, projecting individual sheets of the Fermi surface, such as Raman scattering, add information relevant for the understanding of the superconductivity in the pnictides, which is hardly accessible by probes that yield the integral response of all Fermi-surface sheets.

The multigap behavior shown in Fig. 3(c) yields the best agreement with theoretical predictions,[27] as plotted in Fig. 3(d). In particular, the following features can be reproduced: (i) the superlinear variation and the broad maximum in A_{1g} symmetry, indicating a strong angular variation of the gaps on the α sheets, (ii) the vanishingly small contribution in B_{1g} symmetry due to matrix-element effects, and (iii) the entire B_{2g} spectra, including the sublinear variation below 30 cm^{-1} due to accidental nodes on the β sheets and the logarithmic variation around the cusplike maximum. When we plot the spectra as a function of $\log(|\Omega - \Omega_{max}|/\Omega_{max})$, we find indeed a universal linear variation on either side of the maximum at $\Omega_{max} = 69$ cm^{-1}, which extends over a decade and half a decade on the high- and the low-energy sides, respectively [Figs. 3(e) and 3(f)]. The divergence is cut only by the resolution of the spectrometer.

The sharp structures observed here open up an opportunity to study the effect of impurities. According to our normal-state results but also to transport,[23] the residual scattering rate is on the same order of magnitude as the gap.[24] Disorder is expected to cut the singularity and to open up a finite gap around the nodes.[26,28] To investigate this issue, we have measured $Ba(Fe_{0.915}Co_{0.085})_2As_2$ with a slightly reduced T_c. As shown in Fig. 4, the B_{2g} spectra indicate a finite threshold and a reduced peak height at around 70 cm^{-1}. These results demonstrate that the energy gap can be dramatically affected by sample properties. It is an open question of how the gap and transport dynamics on different portions of the bands and Brillouin zone are modified by doping and disorder. The effects of changes in the pairing interaction and the scattering rates need to be disentangled, which opens an area of further investigation and suggests that a number of apparently contradictory experiments may be reconciled by considering sample quality and distinguishing bulk versus surface sensitive measurements.

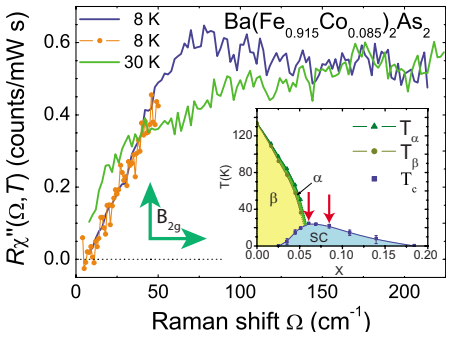

FIG. 4. (Color online) B_{2g} Raman-scattering response $R\chi''(\Omega,T)$ of $Ba(Fe_{0.915}Co_{0.085})_2As_2$. Spectra plotted with full lines [(orange) points] are measured with a resolution of 5.0 cm^{-1} (3.6 cm^{-1}). The inset shows the phase diagram (Ref. 23) with the two samples studied here indicated by arrows. Instead of the sublinear energy dependence at 6.1% [Fig. 3(b)], a finite gap of approximately 10 cm^{-1} is clearly resolved here. The logarithmic singularity is replaced by a broad maximum. Both the low- and the high-energy parts of the spectra follow naturally from the influence of impurities (Ref. 26).

The observed power laws arguing for accidental nodes on the β sheets and near nodes on the α sheets are inconsistent with ARPES (Refs. 14 and 15) but consistent with penetration depth and thermal-conductivity studies.[10,12,16,29] A possible distinction may be made when one considers probing the surface versus probing the bulk as Raman scattering does. Yet, another intriguing possibility is that there may be competing superconducting instabilities that can be triggered by small changes in carrier concentrations. This appears to be the case in several numerical simulations of spin-fluctuation models using both fluctuation exchange in random-phase approximation (Refs. 30 and 31) and numerical functional renormalization-group[32] calculations. These calculations find that s-wave (A_{1g}) and d-wave (B_{2g}) instabilities can occur in multiband models of the Fe-pnictides, which lie relatively close to each other. Moreover, the s-wave pair state is found to have substantial anisotropy. Finally, since our samples are still very close to a spin-density wave (SDW) state, it is plausible that the order parameters for superconductivity and SDW magnetism couple. The resulting apparent gap anisotropy might not exist without SDW order or fluctuations. At the doping level studied, we

could not find indications of collective modes such as proposed for the case of an $s_{\pm}$ state.[33]

Thus, Raman measurements show that for $Ba(Fe_{1-x}Co_x)_2As_2$, different nodal or near-nodal behavior occurs on the α and β Fermi-surface sheets. In either case, impurity scattering is of crucial importance when analyzing the superconducting gap in the pnictides. The polarization dependence of the data both in the superconducting and normal states argues for anisotropic charge dynamics on the different Fermi-surface sheets: a signature of strongly momentum-dependent particle interaction. Nesting properties between the α and β sheets rather than electron-phonon coupling would provide a strongly enhanced dynamic interaction between electrons from nearest-neighbor Fe orbitals. In this way, the iron pnictides would be indeed close relatives of the cuprates, the ruthenates, some heavy-fermion compounds, or even ^{3}He being at the brink of stability of various ground states.[34]

We acknowledge support by the DFG under Grant No. HA 2071/3 via Research Unit FOR538. The work at SLAC and Stanford University is supported by the Department of Energy, Office of Basic Energy Sciences under Contract No. DE-AC02-76SF00515. T.P.D. and R.H. gratefully acknowedge support by the KITP.

[1] Y. Kamihara, T. Watanabe, M. Hirano, and H. Hosono, J. Am. Chem. Soc. **130**, 3296 (2008).
[2] M. Rotter, M. Tegel, and D. Johrendt, Phys. Rev. Lett. **101**, 107006 (2008).
[3] H. Luetkens, H.-H. Klauss, M. Kraken, F. J. Litterst, T. Dellmann, R. Klingeler, C. Hess, R. Khasanov, A. Amato, C. Baines, M. Kosmala, O. J. Schumann, M. Braden, J. Hamann-Borrero, N. Leps, A. Kondrat, G. Behr, J. Werner, and B. Buchner, Nature Mater. **8**, 305 (2009).
[4] H. Chen, Y. Ren, Y. Qiu, W. Bao, R. H. Liu, G. Wu, T. Wu, Y. L. Xie, X. F. Wang, Q. Huang, and X. H. Chen, EPL **85**, 17006 (2009).
[5] T. Goko, A. A. Aczel, E. Baggio-Saitovitch, S. L. Bud'ko, P. C. Canfield, J. P. Carlo, G. F. Chen, P. Dai, A. C. Hamann, W. Z. Hu, H. Kageyama, G. M. Luke, J. L. Luo, B. Nachumi, N. Ni, D. Reznik, D. R. Sanchez-Candela, A. T. Savici, K. J. Sikes, N. L. Wang, C. R. Wiebe, T. J. Williams, T. Yamamoto, W. Yu, and Y. J. Uemura, Phys. Rev. B **80**, 024508 (2009).
[6] D. H. Lu, M. Yi, S.-K. Mo, A. S. Erickson, J. Analytis, J.-H. Chu, D. J. Singh, Z. Hussain, T. H. Geballe, I. R. Fisher, and Z.-X. Shen, Nature (London) **455**, 81 (2008).
[7] E. Z. Kurmaev, R. G. Wilks, A. Moewes, N. A. Skorikov, Y. A. Izyumov, L. D. Finkelstein, R. H. Li, and X. H. Chen, Phys. Rev. B **78**, 220503(R) (2008).
[8] C. C. Tsuei and J. R. Kirtley, Rev. Mod. Phys. **72**, 969 (2000).
[9] J. D. Fletcher, A. Serafin, L. Malone, J. G. Analytis, J.-H. Chu, A. S. Erickson, I. R. Fisher, and A. Carrington, Phys. Rev. Lett. **102**, 147001 (2009).
[10] C. W. Hicks, T. M. Lippman, M. E. Huber, J. G. Analytis, J.-H. Chu, A. S. Erickson, I. R. Fisher, and K. A. Moler, Phys. Rev. Lett. **103**, 127003 (2009).
[11] R. T. Gordon, C. Martin, H. Kim, N. Ni, M. A. Tanatar, J. Schmalian, I. I. Mazin, S. L. Bud'ko, P. C. Canfield, and R. Prozorov, Phys. Rev. B **79**, 100506(R) (2009).
[12] R. Prozorov, M. Tanatar, R. Gordon, C. Martin, H. Kim, V. Kogan, N. Ni, M. Tillman, S. Bud'ko, and P. Canfield, Physica C **469**, 582 (2009).
[13] L. Malone, J. D. Fletcher, A. Serafin, A. Carrington, N. D. Zhigadlo, Z. Bukowski, S. Katrych, and J. Karpinski, Phys. Rev. B **79**, 140501(R) (2009).
[14] D. V. Evtushinsky, D. S. Inosov, V. B. Zabolotnyy, A. Koitzsch, M. Knupfer, B. Buchner, M. S. Viazovska, G. L. Sun, V. Hinkov, A. V. Boris, C. T. Lin, B. Keimer, A. Varykhalov, A. A. Kordyuk, and S. V. Borisenko, Phys. Rev. B **79**, 054517 (2009).
[15] K. Terashima, Y. Sekiba, J. H. Bowen, K. Nakayama, T. Kawahara, T. Sato, P. Richard, Y.-M. Xu, L. J. Li, G. H. Cao, Z.-A. Xu, H. Ding, and T. Takahashi, Proc. Natl. Acad. Sci. U.S.A. **106**, 7330 (2009).
[16] M. Tanatar, J. Reid, H. Shakeripour, X. Luo, N. Doiron-Leyraud, N. Ni, S. Bud'ko, P. Canfield, R. Prozorov, and L. Taillefer, arXiv:0907.1276 (unpublished).
[17] Y.-L. Wang, L. Shan, L. Fang, P. Cheng, C. Ren, and H.-W. Wen, Supercond. Sci. Technol. **22**, 015018 (2009).
[18] T. Kondo, A. F. Santander-Syro, O. Copie, C. Liu, M. E. Tillman, E. D. Mun, J. Schmalian, S. L. Bud'ko, M. A. Tanatar, P. C. Canfield, and A. Kaminski, Phys. Rev. Lett. **101**, 147003 (2008).
[19] P. Samuely, Z. Pribulov, P. Szab, G. Prists, S. Bud'ko, and P. Canfield, Physica C **469**, 507 (2009).
[20] H.-J. Grafe, D. Paar, G. Lang, N. J. Curro, G. Behr, J. Werner, J. Hamann-Borrero, C. Hess, N. Leps, R. Klingeler, and B. Buchner, Phys. Rev. Lett. **101**, 047003 (2008).
[21] H. Mukuda, N. Terasaki, M. Yashima, H. Nishimura, Y. Kitaoka, and A. Iyo, Physica C **469**, 559 (2009).
[22] T. Devereaux and R. Hackl, Rev. Mod. Phys. **79**, 175 (2007).
[23] J.-H. Chu, J. G. Analytis, C. Kucharczyk, and I. R. Fisher, Phys. Rev. B **79**, 014506 (2009).
[24] Details will be presented in an upcoming publication.
[25] The spin-chirality operator, crystal-field excitations, or interorbital transitions can have A_{2g} symmetry. A_{2g} contributions are also expected if the light-scattering process is not invariant under time reversion, for instance, if the photon energy is equal to an interband transition.
[26] T. P. Devereaux, Phys. Rev. Lett. **74**, 4313 (1995).
[27] G. R. Boyd, T. P. Devereaux, P. J. Hirschfeld, V. Mishra, and D. J. Scalapino, Phys. Rev. B **79**, 174521 (2009).
[28] V. Mishra, G. Boyd, S. Graser, T. Maier, P. J. Hirschfeld, and D. J. Scalapino, Phys. Rev. B **79**, 094512 (2009).
[29] V. Mishra, A. Vorontsov, P. Hirschfeld, and I. Vekhter, arXiv:0907.4657 (unpublished).
[30] K. Kuroki, S. Onari, R. Arita, H. Usui, Y. Tanaka, H. Kontani, and H. Aoki, Phys. Rev. Lett. **101**, 087004 (2008).
[31] S. Graser, T. Maier, P. Hirschfeld, and D. Scalapino, New J. Phys. **11**, 025016 (2009).
[32] F. Wang, H. Zhai, and D.-H. Lee, EPL **85**, 37005 (2009).
[33] A. V. Chubukov, I. Eremin, and M. M. Korshunov, Phys. Rev. B **79**, 220501(R) (2009).
[34] P. Monthoux, D. Pines, and G. G. Lonzarich, Nature (London) **450**, 1177 (2007).